J. Cent. South Univ. Technol. (2006)06−0726−07
DOI: 10.1007/s11771−006−0022−8

Behavior of concrete and concrete-filled circular steel tubular stub columns at constant high temperatures

DING Fa-xing(丁发兴), YU Zhi-wu(余志武)

(School of Civil and Architectural Engineering, Central South University, Changsha 410075, China)

Abstract: Based on reanalyzing test results of uniaxial compressive behavior of concrete at constant high temperatures in China, with the compressive cube strength of concrete from 20 to 80 MPa, unified formulas for uniaxial compressive strength, elastic modulus, strain at peak uniaxial compression and mathematical expression for unaxial compressive stress-strain relations for the concrete at constant high temperatures were studied. Furthermore, the axial stress-axial strain relations between laterally confined concrete under axial compression and multiaxial stress-strain relations for steel at constant high temperatures were studied. Finally, based on continuum mechanics, the mechanics model for concentric cylinders of circular steel tube with concrete core of entire section loaded at constant high temperatures was established. Applying elasto-plastic analysis method, a FORTRAN program was developed, and the concrete-filled circular steel tubular (CFST) stub columns at constant high temperatures were analyzed. The analysis results are in agreement with the experiment ones from references.

Key words: concrete; concrete-filled steel tubular column; behavior; high temperature
CLC number: TU352.5 **Document code:** A

1 INTRODUCTION

In the past decade, many experimental researches on the uniaxial compressive behavior of concrete at constant high temperatures or at elevated temperatures have been reported[1−7]. These research achievements are the basis of using the numerical methods for calculation of fire resistance of concrete or concrete-filled circular steel tubular (CFST) structural members.

However, similar to the research methods of mechanical indexes for concrete uniaxial behavior at room temperature[8], researchers in China adopt divisional description for the mechanical indexes at constant high temperatures of normal-strength concrete (with compressive cube strengths f_{cu} up to 60 MPa) and high-strength concrete (with f_{cu} between 60 MPa and 100 MPa). And for each type of concrete, the formulas for mechanical indexes at constant high temperatures were developed, which led to big error of calculation results at divisional borderline. Obviously, these not only cause the confusion of physical concept, but also bring troubles to the fire resistance analysis of concrete structures. After summarizing the test results[1−2] of various concrete grades under the same test equipment and conditions (unstressed tests where the specimens were heated under no initial stress and loaded to failure at the desired constant high temperature after maintained for 6 h), the objective of this research is to propose the unified formulas which can be applied to various grades of concrete at constant high temperatures for uniaxial compressive strength, elastic modulus and strain at peak uniaxial compression and the uniaxial stress-strain relations of concrete various grades at constant high temperatures.

At present, research is very limited on the compressive behavior of CFST stub columns at constant high temperatures with unstressed tests, and only HAN[9] reported 6 specimens. The numerical methods for calculating the behaviors of CFST stub columns at constant high temperatures are the extension at room temperature. A numerical method called combined method presented by HAN[9] was developed for the behavior of the stub columns both at room and constant high temperatures. Another numerical method called elasto-plastic analysis method presented by DING et al[10] was developed for the behavior of the stub columns at room temperature. Another objective of this research is to extend the elasto-plastic analysis method and the corresponding stress-strain relations of materials from room temperature to constant high temperatures, and to achieve elasto-plastic analysis for the behavior of the stub columns at constant high temperatures.

Received date: 2006−03−14; **Accepted date:** 2006−05−02
Foundation item: Projects(50438020; 50578162) supported by the National Natural Sceince Foundation of China
Corresponding author: YU Zhi-wu, Professor; Tel: +86-731-2655366; E-mail: zhwyu@mail.csu.edu.cn

2 MECHANICAL PROPERTIES OF UNIAXIAL COMPRESSIVE CONCRETE

2.1 Uniaxial compressive strength

Fig.1 shows the test results of uniaxial compressive strength of various concrete grades at target temperature to room temperature. With the increase of target temperature, the uniaxial compressive strength ratio f_c^T/f_c tends to decrease as a whole. Experimental studies[1−2] show that for the concrete with f_{cu} between 20 MPa and 40 MPa, at the same target temperature, the loss of uniaxial compressive strength is almost the same, but for higher strength grades of concrete with f_{cu} between 40 MPa and 80 MPa, at the same target temperature, the loss of uniaxial compressive strength increases. From the test results[1−2], through regression analysis, the following unified formula can be obtained:

$$\frac{f_c^T}{f_c}=\frac{1}{1+19\left[(T-293)/900\right]^{b_1}} \tag{1}$$

where f_c^T and f_c are the uniaxial compressive strength of concrete at the target temperature of T and room temperature, respectively, and

$$b_1=\begin{cases}6.70, & 20\le f_{cu}\le 40\,\mathrm{MPa}\\ 3.65+\dfrac{3.05}{1+0.001(f_{cu}-40)^3}, & f_{cu}>40\,\mathrm{MPa}\end{cases}$$

According to Fig.1 and Eqn.(1), the uniaxial compressive strength for various concrete grades at constant high temperatures can be estimated compared with the test results[1−2].

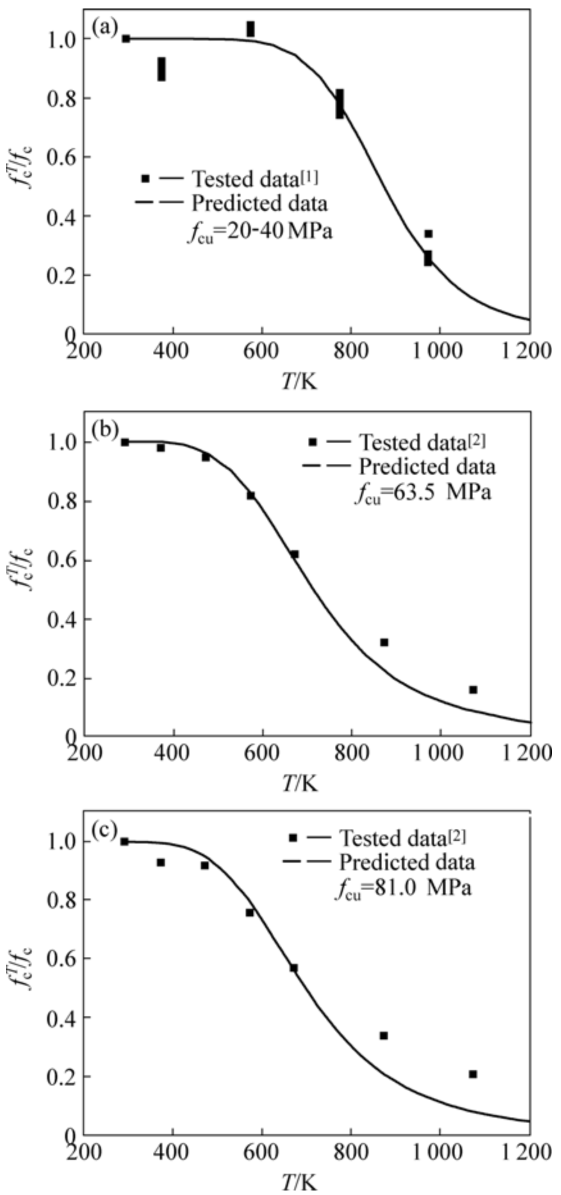

Fig.1 Comparisons between predicted data and tested data of uniaxial compressive strength at constant high temperatures

2.2 Elastic modulus

Fig.2 shows the test results of elastic modulus at target temperature to room temperature of various concrete grades. With the increase of target temperature, the elastic modulus ratio E_c^T/E_c tends to decrease as a whole. Compared with Fig.1, at the same target temperature, the loss of elastic modulus at constant high temperatures is higher than the loss of unixial compressive strength. Experimental studies[1−2] show that the trend of elastic modulus ratio E_c^T/E_c is similar to the uniaxial compressive strength ratio f_c^T/f_c as the strength grades of concrete increase. From the test results[1−2], the following unified formula can be developed:

$$\frac{E_c^T}{E_c}=\frac{1}{1+120\left[(T-293)/900\right]^{b_2}+0.23\left[(T-293)/100\right]^{1.5}} \tag{2}$$

where E_c^T and E_c are the elastic modulus of concrete at the target temperature of T and room temperature, respectively, and

$$b_2=\begin{cases}7.65, & 20\le f_{cu}\le 40\,\mathrm{MPa}\\ 4.60+\dfrac{3.05}{1+0.001(f_{cu}-40)^3}, & f_{cu}>40\,\mathrm{MPa}\end{cases}$$

According to Fig.2 and Eqn.(2), the elastic modulus (dash line) for various concrete grades at constant high temperatures can be estimated compared with the test results[1−2].

2. 3 Strain at peak uniaxial compression

Fig.3 shows the strain at peak uniaxial compression of various concrete grades at target temperature to room

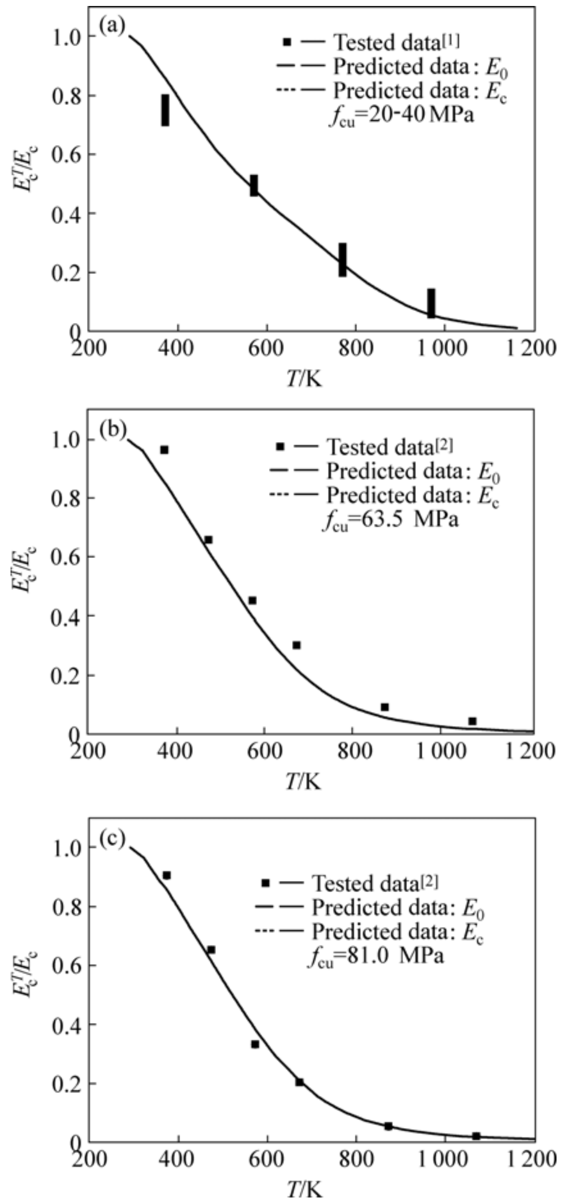

Fig.2 Comparisons between predicted data and tested data of elastic modulus at constant high temperatures

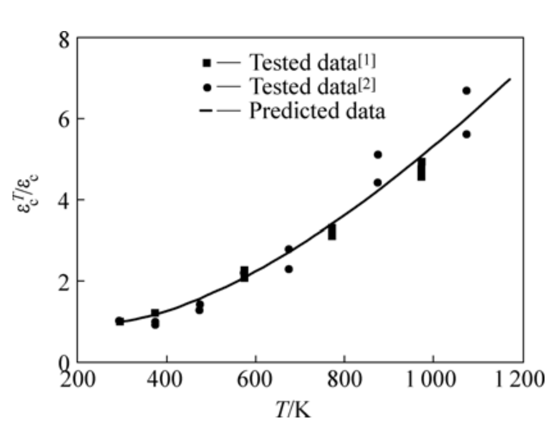

Fig.3 Comparisons between predicted data and tested data of strain at peak uniaxial compression at constant high temperatures

temperature. It can be seen that the strain at peak uniaxial compression ratio $\varepsilon_c^T/\varepsilon_c$ increases as the target temperature increases. At the same target temperature, the influence of strength grade of concrete on $\varepsilon_c^T/\varepsilon_c$ is relatively small. From the test results[1−2], the influence of strength grades of concrete is neglected and the following unified formula can be obtained:

$$\varepsilon_c^T / \varepsilon_c = 1 + 0.23[(T-293)/100]^{1.5} \tag{3}$$

where ε_c^T and ε_c are the strain at peak uniaxial compression of concrete at the target temperature of T and room temperature, respectively.

According to Fig.3 and Eqn.(3), the strain at peak uniaxial compression for various concrete grades at constant high temperatures can be estimated compared with the tested results[1−2].

2.4 Uniaxial compressive stress-strain relations

Test results[1−2] show that the shapes of uniaxial compressive stress-strain relations of concrete at constant high temperatures are similar to that at room temperature. Therefore, the suggested generic forms of mathematical equations[8] for the uniaxial compressive stress-strain relations of various concrete grades at room temperature can also be used at constant high temperatures. The following non-dimensional mathematical form for the uniaxial compressive stress-stain relations of concrete at constant high temperatures can be gotten:

$$y = \begin{cases} \dfrac{Ax - x^2}{1 + (A-2)x^2}, & x \le 1 \\ \dfrac{x}{\alpha(x-1)^2 + x}, & x > 1 \end{cases} \tag{4}$$

where $y=\sigma/f_c^T$; $x=\varepsilon/\varepsilon_c^T$; σ is the compressive stress; ε is the compressive strain. Expressions of $f_c = 0.4 f_{cu}^{7/6}$, $\varepsilon_c = 383\times10^{-6} f_{cu}^{7/18}$, $A_1 = 9.1 f_{cu}^{-4/9}$ and α_1=2.5×10^{-5} f_{cu}^3 were suggested by YU et al[8]. As seen from Fig.2, the predicted curves between the elastic modulus ratio E_c^T/E_c and the secant modulus at the peak stress ratio E_0^T/E_0 ($E_0=f_c/\varepsilon_c$ and $E_0^T=f_c^T/\varepsilon_c^T$, solid line in Fig.2) are almost the same.

Comparisons between the tested data and the predicted data are shown in Fig.4. It can be seen that the model provides an approximation with the right trends of the full uniaxial compressive stress-stain relations for concrete at constant high temperatures.

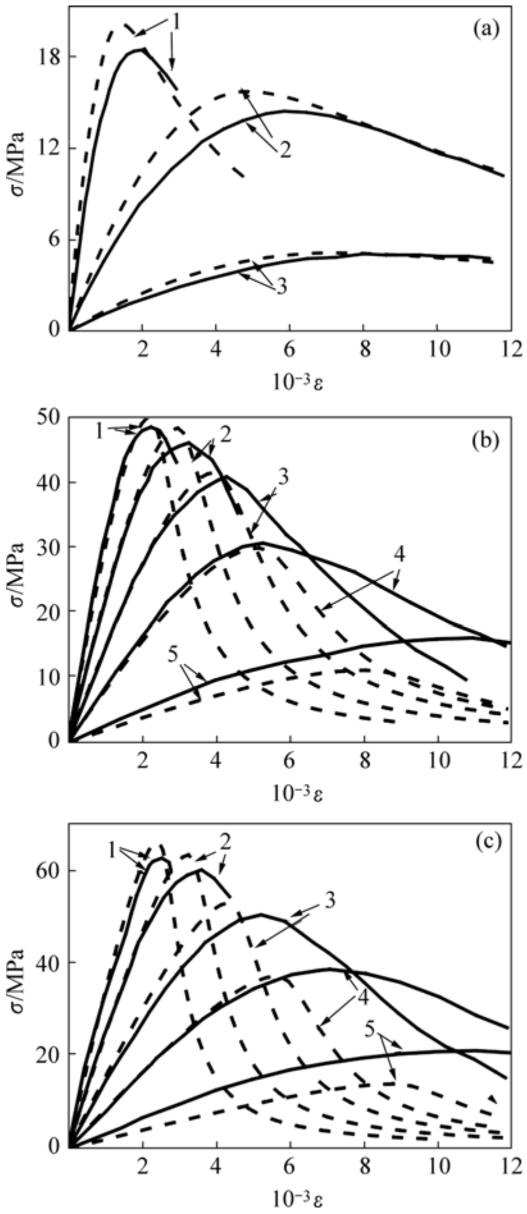

Fig.4 Compressive stress-strain relations of different concrete grades at constant high temperatures
—— — Test curves; - - - — Predict curves
(a) f_{cu} =28.8 MPa[1], 1—293 K, 2—773 K, 3—973 K;
(b) f_{cu} =63.5 MPa[2], 1—373 K, 2—473 K, 3—573 K, 4—673 K, 5—873 K;
(c) f_{cu} =81.0 MPa[2], 1—373 K; 2—473 K; 3—573 K; 4—673 K; 5—873 K

3 ELASTO-PLASTIC ANALYSIS OF CFST STUB COLUMNS

3.1 Basic assumptions

3.1.1 Axial stress-axial strain relations of laterally confined concrete under axial compression at constant high temperatures

Research is very limited on the behavior of the axial stress-axial strain relations for laterally confined concrete under axial compression at constant high temperatures. In order to satisfy the analysis of fire resistance for concrete structures at constant high or elevated temperature, generally, researchers[11] took the following measurements: the mathematical equations of the axial stress-axial strain relations for laterally confined concrete under axial compression at room temperature was kept, in which the expressions of the uniaxial compressive strength and the corresponding strain at room temperature were replaced by the expressions at constant high temperatures. The measurement was also adopt by authors in this study, based on the mathematical equations in Ref. [10], thus the axial stress-axial strain relations and laterally confined concrete under axial compression at constant high temperatures was suggested (seen in Fig.5):

$$y=\begin{cases}\dfrac{A_2^T x-x^2}{1+(A_2^T-2)x}, & x\le 1\\[2ex] \dfrac{x}{\alpha_2^T(x-1)^2+x}, & x>1\end{cases} \tag{5}$$

where $y=\sigma_{L,c}^T/f_c^{*T}$; $x=\varepsilon_{L,c}^T/\varepsilon_f^T$; $\sigma_{L,c}^T$ and f_c^{*T} are axial stress and peak axial stress of concrete, respectively; $\varepsilon_{L,c}^T$ and ε_f^T are axial strain and axial strain at peak axial compression under axial compression and lateral confining at constant high temperature; A_2^T is variable of ascending branch; α_2^T is variable of descending branch of the axial stress-axial strain relations at constant high

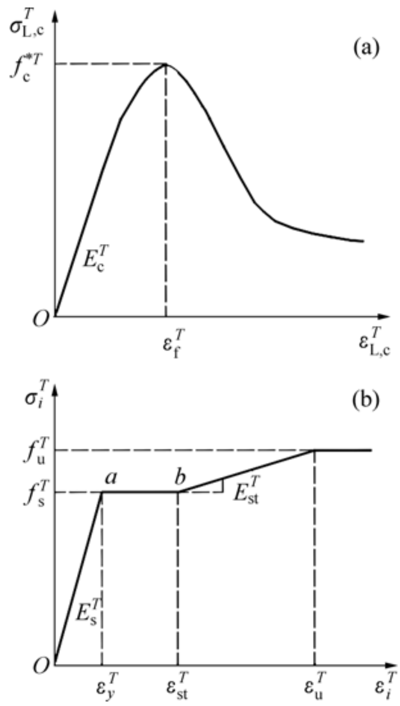

Fig. 5 Stress-stain relations of materials
(a) Concrete; (b) Steel

temperatures, respectively. And

$$\frac{f_{\rm c}^{*T}}{f_{\rm c}^{T}}=1+3.4\frac{\sigma_{\rm r,c}^{T}}{f_{\rm c}^{T}}$$

$$\varepsilon_{\rm f}^{T}=\varepsilon_{0}^{T}(1+3.4\frac{\sigma_{\rm r,c}^{T}}{f_{\rm c}^{T}})\left[1+4.8(A_1-1)(\frac{\sigma_{\rm r,c}^{T}}{f_{\rm c}^{T}})^{0.5}\right]$$

$$A_2^T=A_1\left[1+4.8(A_1-1)(\frac{\sigma_{\rm r,c}^{T}}{f_{\rm c}^{T}})^{0.5}\right]$$

$$\alpha_2^T=\alpha_1\frac{10^{-4}+1.2\times10^4 f_{\rm cu}^{-3}\cdot\sigma_{\rm r,c}^{T}/f_{\rm c}^{T}}{10^{-4}+\sigma_{\rm r,c}^{T}/f_{\rm c}^{T}}$$

where $\sigma_{\rm r,c}^{T}$ is radial stress of concrete.

The expression of the secant concrete Poisson's ratio at constant high temperatures is also similar to that at room temperature[10]:

$$v_{\rm c}^{T}=\begin{cases} v_0,\ x\le1, y\le y_{\rm a} \\ v_{\rm f}-(v_{\rm f}-v_0)\sqrt{1-(\frac{y-y_{\rm a}}{1-y_{\rm a}})^2},\ x\le1, y_{\rm a}\le y\le1 \\ v_{\rm f},\ x>1, y<1 \end{cases} \tag{6}$$

where v_0 and $v_{\rm f}$ are the initial Poisson's ratio and secant value of Poisson's ratio at peak axial compression, and v_0=0.2, $v_{\rm f}$=1−0.0025($f_{\rm cu}$−20), $y_{\rm a}$=0.3+0.002($f_{\rm cu}$−20).

3.1.2 Multiaxial stress-strain relations of steel at constant high temperatures

Research is also very limited on the behaviors of the steel multiaxial stress-strain relations at constant high temperatures. Generally, the plasto elasticity theory also can be used to multiaxial stress-strain relations for steel material at constant high temperatures. Thus the multiaxial stress-strain relations for steel at constant high temperatures can be obtained when the expression for stress-strain relations of steel at room temperature was kept, in which the yield strength and Young's modulus at room temperature were replaced. The reduction factors of yield strength and Young's modulus of steel at constant high temperatures recommended in Eurocode 3 were quoted as seen in Table 1.

Based on the mathematical equations of steel at room temperature in Ref.[10], the multiaxial stress-strain relations for steel at constant high temperatures was presented (seen in Fig.5(b)):

$$\sigma_i^T=\begin{cases} E_{\rm s}^T\varepsilon_i^T,\varepsilon_i^T\le\varepsilon_{\rm y}^T \\ f_{\rm s}^T,\varepsilon_{\rm y}^T<\varepsilon_i^T\le\varepsilon_{\rm st}^T \\ f_{\rm s}^T+\zeta E_{\rm s}^T(\varepsilon_i^T-\varepsilon_{\rm st}^T),\ \varepsilon_{\rm st}^T<\varepsilon_i^T\le\varepsilon_{\rm u}^T \\ f_{\rm u}^T,\varepsilon_i^T>\varepsilon_{\rm u}^T \end{cases} \tag{7}$$

where σ_i^T, $f_{\rm s}^T$ and $f_{\rm u}^T$ are equivalent stress, yield strength and tensile strength of steel at constant high temperature, respectively; $f_{\rm u}^T=1.5f_{\rm s}^T$; $E_{\rm s}^T$ and $E_{\rm st}^T$ are Young's modulus and harden modulus of steel at constant high temperatures, respectively; $\varepsilon_{\rm st}^T=12\varepsilon_y^T$, $\varepsilon_{\rm u}^T=120\varepsilon_y^T$ and $E_{\rm st}^T=\zeta E_{\rm s}^T=(1/216)E_{\rm s}^T$.

Table 1 Reduction factor of yield strength and elastic modulus of steel at constant high temperatures

T/K	$f_{\rm s}^T/f_{\rm s}$	$E_{\rm s}^T/E_{\rm s}$
293	1.000	1.000
373	1.000	1.000
473	1.000	0.900
573	1.000	0.800
673	1.000	0.700
773	0.780	0.600
873	0.470	0.310
973	0.230	0.130
1073	0.110	0.090
1173	0.060	0.068
1273	0.040	0.045
1373	0.020	0.023
1473	0	0

Note: $f_{\rm s}$ and $E_{\rm s}$ are yield strength and Young's modulus of steel at room temperature, respectively, $E_{\rm s}$=2.06×10^5 MPa

Expression of the secant Poisson's ratio for steel at constant high temperatures ($v_{\rm s}^T$) is also similar to that at room temperature[10]:

$$v_{\rm s}^T=\begin{cases} 0.285,\ \varepsilon_i^T\le0.8\varepsilon_y^T \\ 1.075(\sigma_i^T/f_{\rm s}^T-0.8)+0.285,\ 0.8\varepsilon_y^T<\varepsilon_i^T<\varepsilon_y^T \\ 0.5,\ \varepsilon_i^T>\varepsilon_y^T \end{cases} \tag{8}$$

3.1.3 Cross-sectional compatible conditions

Before being loaded, suppose the temperatures within steel tube concrete core were the same. The influence of temperature on the axial and radial swelling deformations of steel tube and concrete core, and body stress of the stub column caused by the temperature were neglected. Complete interaction and no slip between the steel tube and concrete core existed through the full range of loading. The interface is continuous and the cross-sectional deformation is compatible.

3.2 Theoretical model

A numerical model called elasto-plastic analysis method was developed for the behavior of CFST stub columns at room temperature. The model for the behavior of CFST stub columns at constant high temperature was an extension of the former model, which was presented by DING et al[10]. Based on continuum mechanics shown in Fig.6, the mechanical model of concentric cylinders of circular steel tube with concrete core of entire section loaded at constant high temperatures was established. In Fig. 6, L is length of cylinder, D is diameter of cylinder, r is radius of concrete core, h is thickness of steel tube and N is axial load. The expressions for composite stress, several internal stresses and corresponding strains of CFST stub columns at constant high temperatures were given as follows.

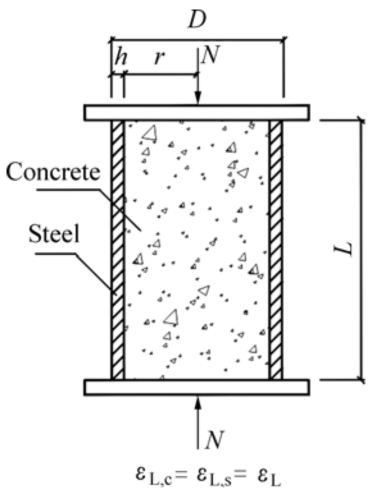

Fig. 6 Mechanical model of the stub column

The composite stress ($f_{\rm sc}^T$)-strain ($\varepsilon_{\rm L}^T$) relations of CFST stub columns at constant high temperatures in elastic stage is:

$$f_{\rm sc}{}^T = E_{\rm sc}{}^T \varepsilon_{\rm L}{}^T \tag{9}$$

where $E_{\rm sc}^T$ is composite modulus of CFST stub columns at constant high temperatures, and

$$E_{\rm sc}^T = (1-\rho)E_{\rm c}^T + \rho E_{\rm s}^T + 2(v_{\rm c}^T - v_{\rm s}^T)^2 (1-\rho)\rho Q^T E_{\rm s}^T \tag{10}$$

where ρ is the cross-sectional steel ratio, $\rho = A_{\rm s}/A_{\rm sc} \approx 4h/D$; $A_{\rm s}$ and $A_{\rm sc}$ are the cross-sectional area of steel tube and total, respectively, and

$$Q^T = \left\{\left[1 - v_{\rm c}^T - 2(v_{\rm c}^T)^2\right] n^T \rho + \left[2 - (v_{\rm s}^T)^2 - \rho + \rho v_{\rm s}^T + \rho (v_{\rm s}^T)^2\right]\right\}^{-1}, n^T = E_{\rm s}^T / E_{\rm c}^T$$

The radial stress ($\sigma_{\rm r,c}^T$), perimeter stress ($\sigma_{\theta,\rm c}^T$) and axial stress ($\sigma_{\rm L,c}^T$) of concrete core at constant high temperatures are:

$$\begin{cases} \sigma_{\rm r,c}^T = \sigma_{\theta,\rm c}^T = \rho (v_{\rm c}^T - v_{\rm s}^T) Q^T E_{\rm s}^T \varepsilon_{\rm L}^T \\ \sigma_{\rm L,c}^T = [E_{\rm c}^T + 2\rho v_{\rm c}^T (v_{\rm c}^T - v_{\rm s}^T) Q^T E_{\rm s}^T] \varepsilon_{\rm L}^T \end{cases} \tag{11}$$

The radial strain ($\sigma_{\rm r,c}^T$) and the perimeter strain ($\sigma_{\theta,\rm c}^T$) of concrete core at constant high temperatures are:

$$\varepsilon_{\rm r,c}^T = \varepsilon_{\theta,\rm c}^T = \left\{\rho \left[1 - v_{\rm c}^T - 2(v_{\rm c}^T)^2\right] (v_{\rm c}^T - v_{\rm s}^T) Q^T n^T - v_{\rm c}^T \right\} \cdot \varepsilon_{\rm L}^T \tag{12}$$

The radial stress ($\sigma_{\rm r,s}^T$), perimeter stress ($\sigma_{\theta,\rm s}^T$) and axial stress ($\sigma_{\rm L,s}^T$) of steel tube at constant high temperatures are:

$$\begin{cases} \sigma_{\rm r,s}^T = [(D/2r)^2 - 1](v_{\rm c}^T - v_{\rm s}^T)(1-\rho) Q^T E_{\rm s}^T \varepsilon_{\rm L}^T \\ \sigma_{\theta,\rm s}^T = -[(D/2r)^2 + 1](v_{\rm c}^T - v_{\rm s}^T)(1-\rho) Q^T E_{\rm s}^T \varepsilon_{\rm L}^T \\ \sigma_{\rm L,s}^T = [1 - 2v_{\rm s}^T (v_{\rm c}^T - v_{\rm s}^T)(1-\rho) Q^T] E_{\rm s}^T \varepsilon_{\rm L}^T \end{cases} \tag{13}$$

The radial strain ($\varepsilon_{\rm r,s}^T$) and perimeter strain ($\varepsilon_{\theta,\rm s}^T$) of steel tube at constant high temperatures are:

$$\begin{cases} \varepsilon_{\rm r,s}^T = \left\{\left[D/(2r)\right]^2 (1 + v_{\rm s}^T) - \left[1 - v_{\rm s}^T - (v_{\rm s}^T)^2\right]\right\} \cdot \\ \quad (1-\rho)(v_{\rm c}^T - v_{\rm s}^T) Q^T \varepsilon_{\rm L}^T - v_{\rm s}^T \varepsilon_{\rm L}^T \\ \varepsilon_{\theta,\rm s}^T = -\left\{\left[D/(2r)\right]^2 (1 + v_{\rm s}^T) + \left[1 - v_{\rm s}^T - (v_{\rm s}^T)^2\right]\right\} \cdot \\ \quad (1-\rho)(v_{\rm c}^T - v_{\rm s}^T) Q^T \varepsilon_{\rm L}^T - v_{\rm s}^T \varepsilon_{\rm L}^T \end{cases} \tag{14}$$

The composite stress ($f_{\rm sc}^T$)-strain ($\varepsilon_{\rm L}^T$) relations of CFST stub columns at constant high temperatures in elasto-plastic stage is:

$$f_{\rm sc}^T = E_{\rm sc}^{tT} \varepsilon_{\rm L}^T \tag{15}$$

where

$$E_{\rm sc}^{\rm t\,T} = (1-\rho)E_{\rm c}^{tT} + \rho E_{\rm s}^{tT} + 2(v_{\rm c}^T - v_{\rm s}^T)^2 (1-\rho)\rho Q_{\rm t}^T E_{\rm s}^{\rm t\,T}$$

The stresses of steel tube at constant high temperatures after yield are:

$$\begin{cases} \sigma_{\theta,\rm s}^T = -2(v_{\rm c}^T - v_{\rm s}^T)(1-\rho) Q_{\rm t}^T E_{\rm s}^{\rm t\,T} \varepsilon_{\rm L}^T \\ \sigma_{\rm L,s}^T = [1 - 2v_{\rm s}^T (v_{\rm c}^T - v_{\rm s}^T)(1-\rho) Q_{\rm t}^T] E_{\rm s}^{\rm t\,T} \varepsilon_{\rm L}^T \end{cases} \tag{16}$$

where

$$Q_{\rm t}^T = \left\{\left[1 - v_{\rm c}^T - 2(v_{\rm c}^T)^2\right] n^T \rho + \left[2 - (v_{\rm s}^T)^2 - \rho + \rho v_{\rm s}^T + \rho (v_{\rm s}^T)^2\right]\right\}^{-1};$$

$$n_{\rm t}^T = E_{\rm s}^{\rm t\,T} / E_{\rm c}^{\rm t\,T}$$

$$E_{\rm c}^{\rm t\,T} = E_{\rm t}^T - 2\rho v_{\rm c}^T (v_{\rm c}^T - v_{\rm s}^T) Q_{\rm t}^T E_{\rm s}^{\rm t\,T}$$

$E_{\rm t}{}^T$ is secant modulus of concrete.

The strains in middle shell of steel tube at constant high temperatures after yield are:

$$\begin{cases} \varepsilon_{\mathrm{r,s}}^T = \left\{ \left(1+v_{\mathrm{s}}^T\right)/(1-\rho/4) - \left[1-v_{\mathrm{s}}^T-(v_{\mathrm{s}}^T)^2\right] \right\} \cdot \\ \qquad (1-\rho)(v_{\mathrm{c}}^T - v_{\mathrm{s}}^T) Q_{\mathrm{t}}^T \varepsilon_{\mathrm{L}}^T - v_{\mathrm{s}}^T \varepsilon_{\mathrm{L}}^T \\ \varepsilon_{\theta,\mathrm{s}}^T = -\left\{ \left(1+v_{\mathrm{s}}^T\right)/(1-\rho/4) + \left[1-v_{\mathrm{s}}^T-(v_{\mathrm{s}}^T)^2\right] \right\} \cdot \\ \qquad (1-\rho)(v_{\mathrm{c}}^T - v_{\mathrm{s}}^T) Q_{\mathrm{t}}^T \varepsilon_{\mathrm{L}}^T - v_{\mathrm{s}}^T \varepsilon_{\mathrm{L}}^T \end{cases} \tag{17}$$

3.3 Example

A computer program for the behavior of CFST stub columns at constant high temperature was developed, which was written in FORTRAN90. The validation of the computer program was achieved through verification against the test results[9]. The comparisons of axial load (N, $N=f_{\mathrm{sc}}{}^T A_{\mathrm{sc}}$)-axial strain ($\varepsilon_L{}^T$) relations between predicted curves and test ones of the CFST stub columns at constant high temperatures are shown in Fig.7. For the temperature up to 873 K, the predicted curves can be used to estimate the test ones. However, the test axial stiffness of the stub columns is lower than the predicted ones, which may be caused by test method of strain at constant high temperatures. For the temperature beyond 1 173 K, the loss of the strength of materials is very great. Though the predicted curve is relatively lower than the test one, the influences on the structural behavior are small.

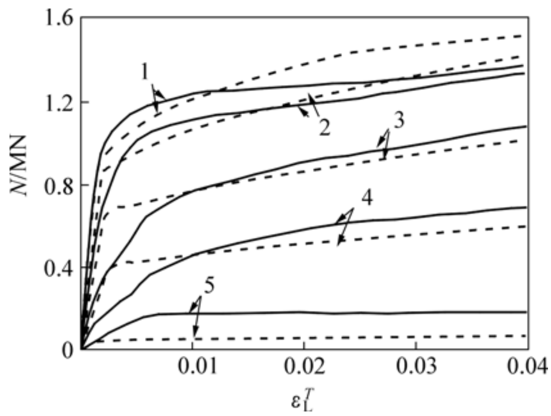

—— — Tested curves; - - — Predicted curves

D=133 mm, h=4.5 mm, L=399 mm, f_{s}=324 MPa, f_{cu}=38.9 MPa[6]

T/K: 1—293; 2—573; 3—773; 4—873; 5—1 173

Fig.7 Comparisons between predicted curves and test ones of columns at constant high temperatures

4 CONCLUSIONS

1) The unified formulas which can be applied to various concrete grades were suggested at constant high temperatures for uniaxial compressive strength, elastic modulus and strain at peak uniaxial compression, and the uniaxial compressive stress-strain relations of various grades of concrete at constant high temperatures were obtained. These unified formulas can be used to predict the test results as a whole.

2) The material constitutive models of both concrete and steel, and elasto-plastic analysis method for the CFST stub columns at constant high temperature were also proposed, which can be used to predict the test data fairly well. Furthermore, research achievements in this paper will provide reference for the further non-linear finite element analysis of CFST columns in fire or at elevated temperatures.

REFERENCES

[1] LI Wei, GUO Zhen-hai. Experimental research of strength and deformation of concrete at high temperature[J]. Journal of Building Structures, 1993, 14(1): 8−16.(in Chinese)

[2] HU Hai-tao, DONG Yu-li. Experimental research on strength and deformation of high-strength concrete at high temperature[J]. China Civil Engineering Journal, 2002, 35(6): 44−47.(in Chinese)

[3] GUO Zhen-hai, SHI Xu-dong. Behavior of reinforced concrete at high temperature and its calculation[M]. Beijing: Tsinghua University Press, 2003.(in Chinese)

[4] Abe T, Furumura F. Mechanical properties of high strength concrete at high temperatures[J]. Journal of Structural Construction Engineering, AIJ, 1999, 515(1): 163−168.(in Japanese)

[5] Castillo C, Duttani A J. Effect of transient high temperature on high-strength concrete[J]. ACI Material Journal, 1990, 87(1): 47−53.

[6] Cheng F P, Kodur V K R, Wang T C. Stress-strain curves for high strength concrete at elevated temperatures[J]. Journal of Materials in Civil Engineering, ASCE, 2004, 16(1): 84−90.

[7] Khalaf F M, Devenny A S. Performance of brick aggregate concrete at high temperatures[J]. Journal of Materials in Civil Engineering, ASCE, 2004, 16(6): 556−565.

[8] YU Zhi-wu, DING Fa-xing. Unified calculation method of compressive mechanical properties of concrete[J]. Journal of Building Structures, 2003, 24(4): 41−46.(in Chinese)

[9] HAN Lin-hai. Concrete filled steel tubular structure [M]. Beijing: Science Press, 2000.(in Chinese)

[10] DING Fa-xing, YU Zhi-wu. Theoretical analysis of mechanical properties of concrete filled tubular steel stub columns[J]. Engineering Mechanics, 2005, 22(1): 173−181.(in Chinese)

[11] JIANG Shou-chao, LI Guo-qiang, LOU Guo-biao, et al. Numerical approach of behavior of steel-concrete composite slabs subjected to fire[J]. Journal of Building Structures, 2004, 25(3): 38−44. (in Chinese)

(Edited by CHEN Can-hua)